The First Organically Templated Layered Iron Phosphate: Hydrothermal Synthesis, Structure, Magnetic Properties, and the Mössbauer Spectrum of [H₃NCH₂CH₂NH₃]₀.₅[Fe(OH)(PO₄)]

Jeffrey R. D. DeBord,*·† William M. Reiff,‡ Robert C. Haushalter,† and Jon Zubieta,*

*Department of Chemistry, Syracuse University, Syracuse, New York 13244; †NEC Research Institute, 4 Independence Way, Princeton, New Jersey 08540; and ‡Department of Chemistry, Northeastern University, Boston, Massachusetts 02115

The first organically templated, layered iron phosphate [H₃NCH₂CH₂NH₃]₀.₅[Fe(OH)(PO₄)], **1**, has been prepared and characterized via single crystal X-ray diffraction, variable temperature magnetic susceptibility measurements, and Mössbauer spectroscopy. Phosphate **1** is synthesized from the hydrothermal reaction of $FeCl_3$, H_3PO_4, ethylenediamine, and H_2O in the mole ratio 1:3.6:4.2:444 for 64 h at 160°C and exhibits a layered structure consisting of infinite chains of edge-sharing {FeO₆} octahedra linked into finite 2-D sheets by {PO₄} tetrahedra that possess terminal P=O groups which protrude into the interlamellar space. The infinite edge-sharing chains display a pairwise puckering resulting from the presence of *trans* μ^2-OH groups arranged in a zig-zag fashion along the chain. The charge compensating ethylenediammonium cations contact both adjacent layers via an elaborate and complicated hydrogen bonded network. Crystal data for **1**: $FePO_5NCH_6$, monoclinic, space group $P2_1/c$, $a = 4.5010(7)$ Å, $b = 6.114(1)$ Å, $c = 18.460(3)$ Å, $\beta = 94.59(1)°$, $V = 56.4(1)$ Å, $Z = 2$, $d_{calc} = 2.608$ g·cm⁻³; 1650 reflections, $R = 0.049$. Variable temperature Mössbauer data, dc magnetization, and ac susceptibility measurements show that **1** undergoes a transition to a weak ferromagnetic state near 30 K. © 1996 Academic Press, Inc.

INTRODUCTION

The widespread applications of zeolites in ion exchange, as sorbents and molecular sieves, and in heterogeneous catalysis (1–3) have stimulated an interest in the synthesis of novel materials with layered and open-framework structures (4). While structures constructed from linked tetrahedra of Si and Al represent the most well developed classes of materials, microporous materials containing other elements have been synthesized in recent years and include the gallophosphate cloverite (5), germanium dioxides (6), and beryllium and zinc phosphates (7). Open-framework structures with transition metal phosphates have been reported for iron (8), cobalt (4), and molybdenum (9).

Frameworks composed of vanadium phosphates have been a particularly fertile source of topologically unique oxide arrays which contain entrained organic (10), inorganic (11), or mixed organic–inorganic cationic templates (12). Synthetic iron phosphates are of particular interest by virtue of applications to the selective oxidation of methanol (13) as well as for the diversity of their structural chemistry and magnetic properties (14). Naturally occurring iron phosphate minerals (15) have been found to provide, primarily through the work of Moore, a large number of structurally diverse examples of both open and dense octahedral–tetrahedral frameworks. Among the most notable of these structures are the gigantic tunnels of ca. 14 Å found in the ferric phosphate cacoxenite (16).

We have recently demonstrated that, by exploiting the presence of cationic organic templates in hydrothermal preparations of *d*-block metal phosphates, a very large variety of metastable phases with layered and open frameworks could be isolated. In many of these cases, the specific, unique material synthesized depends upon the exquisitely sensitive relationship between the charge, shape, and volume of the cationic template to the nature of the void formed in the anionic framework. Complex hydrogen bonding between protonated amine templates and framework oxygen atoms has been shown to be a particularly influential factor in the determining which material will craystallize under given conditions. Because it takes a relatively large number of framework atoms to completely encapsulate the bulky organic templates, as compared to cations like the alkali metals, there is a corresponding increase in the size and complexity of the framework upon increasing the size of the template. Also, since the transition elements do not display tetrahedral coordination in these materials, none of the frameworks obtained resemble those found in the all tetrahedral framework zeolites and aluminophosphates. By applying these techniques to the iron phosphate system, the first example

TABLE 1
Experimental Conditions and Crystal Data for the X-Ray Diffraction Study of $[H_3NCH_2CH_2NH_3]_{0.5}[Fe(OH)(PO_4)]$ (1)

Empirical formula	$FePO_5NCH_6$
FW(g/mol)	198.88
Crystal color, habit	orange, prism
Crystal dimensions (mm)	$0.20 \times 0.10 \times 0.10$ mm
Crystal system	monoclinic
Space group	$P2_1/c$ (#14)
Lattice parameters	$a = 4.5010(7)$ Å
	$b = 6.114(1)$ Å
	$c = 18.460(3)$ Å
	$\beta = 94.59(1)°$
	$V = 506.4(1)$ Å
Z	4
D_{calcd} (g · cm⁻³)	2.608 (g · cm⁻³)
Diffractometer	Rigaku AFC7R
Scan type	$\omega - 2\theta$
2θ(max) (deg)	60.1°
Observed reflections ($I > 3.00\ \sigma(I)$)	1089
No. of variables	82
Reflection/parameter ratio	13.28
R; R_w	0.049; 0.056
Goodness of fit	2.77
Max shift/error in final cycle	0.00
Maximum peak in final diff. map	0.88 e⁻/Å³
Minimum peak in final diff. map	−0.93 e⁻/Å³

of an organically templated layered iron phosphate phase $[H_3NCH_2CH_2NH_3]_{0.5}[Fe(OH)(PO_4)]$, **1**, has been isolated and structurally characterized.

EXPERIMENTAL

Synthesis. The hydrothermal syntheses were carried out in polytetrafluoroethylene-lined stainless steel containers under autogeneous pressures with 30–50% fill volumes. The reaction of $FeCl_3$, H_3PO_4, ethylenediamine, and H_2O

TABLE 2
Atomic Coordinates and Temperature Factors (B_{eq}) for $[H_3NCH_2CH_2NH_3]_{0.5}[Fe(OH)(PO_4)]$ (1)

Atom	x	y	z	$B_{eq}{}^a$
Fe(1)	−0.5033(2)	−01431(1)	0.24627(4)	0.79(1)
P(1)	0.0106(3)	0.0994(2)	0.34533(7)	0.73(2)
O(1)	−0.8272(8)	−0.1894(6)	0.1693(2)	1.08(7)
O(2)	−0.7315(8)	0.1047(5)	0.2925(2)	0.86(6)
O(3)	−0.1762(8)	−0.1052(5)	0.3248(2)	1.05(7)
O(4)	−0.3526(8)	0.1105(5)	0.1933(2)	0.82(6)
O(5)	0.1392(8)	0.0841(6)	0.4227(2)	1.27(7)
N(1)	−0.5557(10)	0.2647(8)	0.0480(2)	1.43(9)
C(1)	−0.395(1)	0.0890(8)	0.0128(3)	1.5(1)

$^a B_{eq} = \frac{8}{3} \pi 2(U_{11}(aa^*)^2 + U_{22}(bb^*)^2 + U_{33}(cc^*)^2 + 2U_{12}aa^*bb^*\cos\gamma + 2U_{13}aa^*cc^* \cos\beta + 2U_{23}bb^*cc^* \cos\alpha)$.

TABLE 3
Selected Bond Lengths (Å) for $[H_3NCH_2CH_2NH_3]_{0.5}[Fe(OH)(PO_4)]$

Atom	Atom	Distance	Atom	Atom	Distance
Fe(1)	O(1)	1.973(4)	Fe(1)	O(2)	2.054(3)
Fe(1)	O(2)	2.032(3)	Fe(1)	O(3)	1.995(4)
Fe(1)	O(4)	1.980(3)	Fe(1)	O(4)	2.012(3)
P(1)	O(3)	1.538(4)	P(1)	O(5)	1.500(4)
			N(1)	C(1)	1.475(7)

in the mole ratio $1:3.6:4.2:444$ at 160° C for 64 h produced $[H_3NCH_2CH_2NH_3]_{0.5}[Fe(OH)(PO_4)]$, **1**, as yellowish prismatic crystals. The optimal conditions required addition of $FeCl_3$ (0.27 g, 1.66 mmol) to the 23 ml PTFE-lined acid digestion bomb followed by H_2O (8 ml, 737 mmol). Upon addition of ethylenediamine (0.28 ml, 6.97 mmol) and H_3PO_4 (0.21 ml, 5.98 mmol) and thorough stirring, the solution pH was 8.0. Upon completion of the reaction and cooling to room temperature, greenish-yellow crystals of **1** were collected, washed with water, and air dried to give a 50% yield based on iron. The material is single phase as judged by comparison of the powder X-ray diffraction of the bulk material to the pattern simulated from the coordinates derived from the single crystal study.

Crystallgraphy. The data were collected at room temperature on a Rigaku AFC7R diffractometer equipped with an 18 kW rotating anode molybdenum target. The data collection parameters and other experimental information are given in Table 1, the fractional coordinates are in Table 2, and some important bond distancs are in Table 3.

Mössbauer. Variable temperature Mössbauer spectra were recorded using equipment that was previously described (17). α-Iron foil was employed as the standard. The spectra were fitted to Lorentzians, using a program written primarily by Stone (18).

Magnetization. The ac susceptibility measurements were performed using a Lakeshore Cryogenics Series 7000 susceptometer applying an ac field of 1 Oe at a frequency of 125 Hz.

RESULTS AND DISCUSSION

Since pH has often proven to be an extremely important factor influencing the growth of specific phases under hydrothermal conditions, we chose a pH near those found in naturally occurring mineral environments which were neutral to slightly alkaline. For the preparation **1**, the reaction of $FeCl_3$, H_3PO_4, ethylenediamine, and H_2O in the mole ratio $1:3.6:4.2:444$ at 160°C for 64 h yielded a single phase product. The pH of the reaction mixture before heating was about 8.
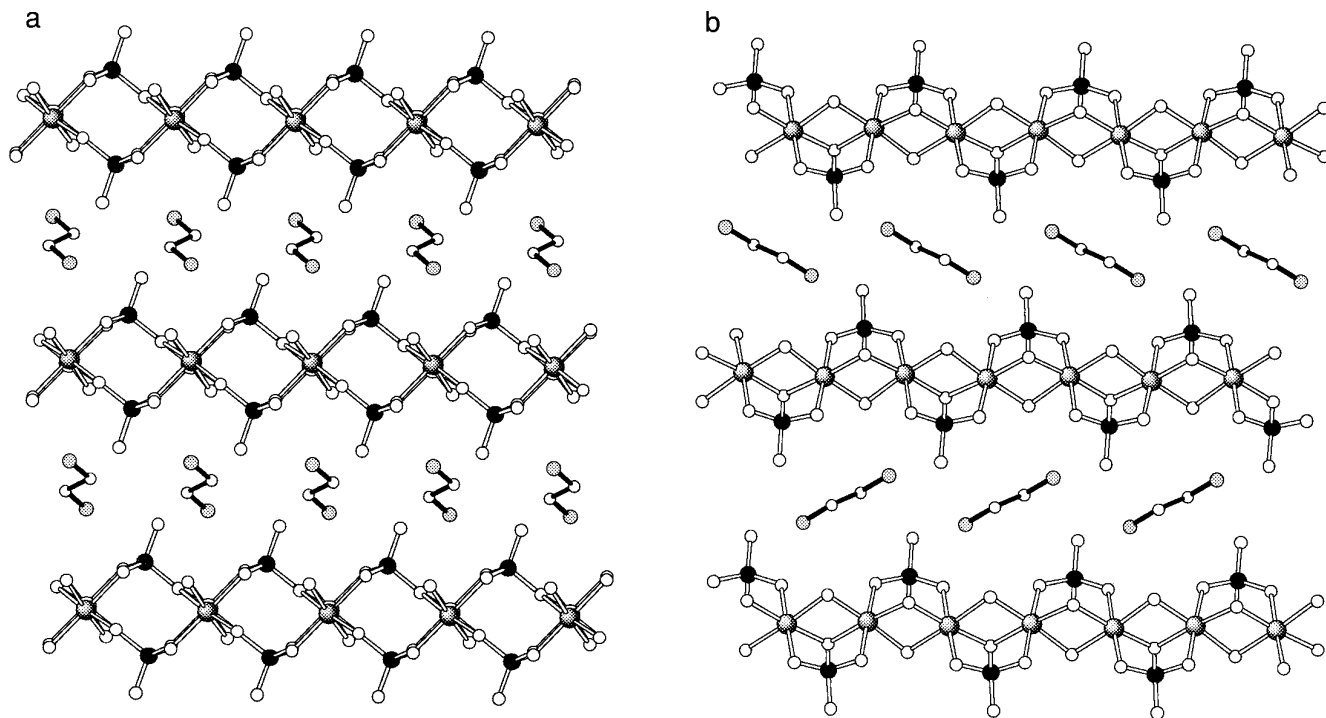
FIG. 1. Two views of the structure of **1** viewed down (a) the **b** axis and (b) the **a** axis showing the interlayer ethylenediammonium cations.

As shown in Figs. 1a and 1b, the structure of **1** consists of inorganic Fe–O–P layers which contain equal numbers of FeO_6 octahedra and PO_4 tetrahedra separated by the organodiammonium cations. The layers are constructed from linear chains of *trans* edge-sharing $\{FeO_6\}$ octahedra, which are linked into the infinite two-dimensional (2-D) sheet through phosphate tetrahedra as shown in Fig. 2.

The geometry at the Fe(III) sites is defined by two bridging –OH groups and four oxygen donors from each of four phosphate tetrahedra. The *trans* orientation of the bridging hydroxyl groups produces a zig-zag $\{Fe–O(H)–Fe–O(H)–\}$ backbone to the linear chain of $\{FeO_6\}$ octahedra as depicted in Fig. 3.

The phosphate groups coordinate to the Fe centers through three oxygen donors; the fourth oxygen is present as a pendant $\{P=O\}$ unit and projects into the interlamellar region. Two of the phosphate oxygen donors of a given $(PO_4)^{3-}$ group bond to each of two adjacent Fe sites of a single chain in the common symmetrically bridging mode, while the third serves to bridge to the adjacent linear array of $\{FeO_6\}$ octahedra through a μ^3 coordination to two adjacent iron sites of the chain. The phosphate tetrahedra linking adjacent chains direct their pendant $\{P=O\}$ groups alternately above and below the plane. The result, as shown

FIG. 2. Polyhedral representation of a layer found in **1** depicting the 1-D chains of edge-sharing octahedra.
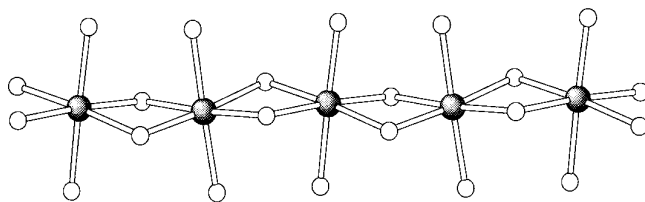

FIG. 3. View of several adjacent FeO_6 octahedra illustrating the pairwise canting.
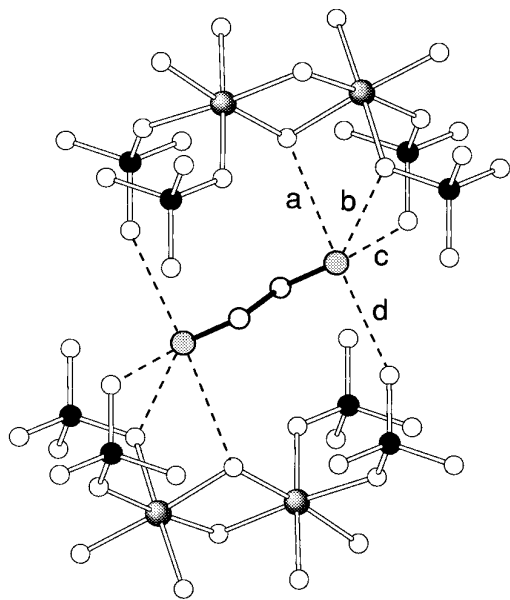
FIG. 4. Illustration of the manner in which the centrosymetric ethylenediammonium cations are hydrogen bonded to the oxide framework of **1**. Distances are: (a) N(1)–O(4) = 2.920(6) Å, (b) N(1)–O(3) = 2.838(6) Å, (c) N(1)–O(5) = 2.730(6) Å, and (d) N(1)–O(5) = 2.755(6) Å.

in Fig. 1, is an inorganic layer three polyhedra in thickness. The projection of the {P=O} into the interlamellar region also serves to provide distinct channels, occupied by the ethylenediammonium cations. The ethylenediammonium cation is snugly and precisely nested via a complicated hydrogen bonded network into its oxide cavity as illustrated in Fig. 4. This extensive hydrogen bonding network likely plays an important role in determining precisely
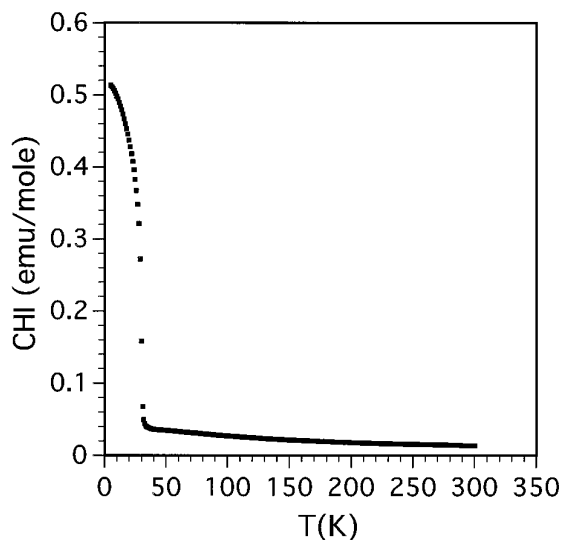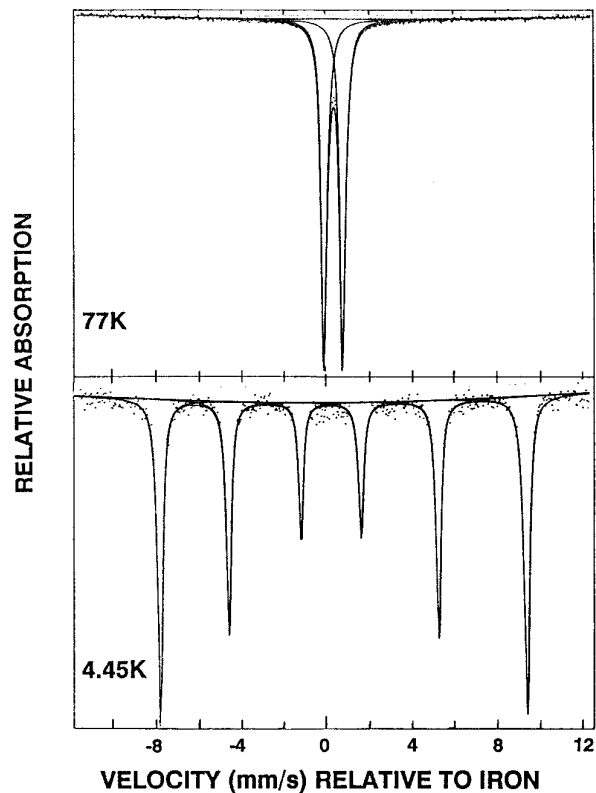

FIG. 6. The ^{57}Fe Mössbauer spectrum of **1** at (a) 77 K and (b) 4.45 K.

which species is least soluble under the given hydrothermal conditions.

The 1-D chains of edge-sharing FeO$_6$ octahedra within the layers of **1** give rise to interesting magnetic behavior from the interactions of adjacent high spin $3d^5$ Fe^{3+} centers. Preliminary dc magnetization measurements, which yielded μ_{eff} (300 K) = 5.77 μ_B consistent with high spin $S = 5/2$ Fe^{3+}, indicated a magnetic ordering in the vicinity of 30 K as shown in Fig. 5. Also apparent is the fact that $\chi^{-1}(T)$ above T_c is linear, which is indicative of paramagnetism, and the value of $\theta = -107$ K suggests rather strong antiferromagnetic interactions between Fe neighbors. In order to elucidate the nature of this transition, variable temperature Mössbauer and ac susceptibility measurements were carried out. Lorentzian fits of the Mössbauer spectra of the title compound at 77 and 4.45 K are shown in Fig. 6. The rapidly relaxing paramagnetic phase corresponds to a single quadrupole doublet consistent with a unique Fe environment whose Mössbauer parameters are typical of high spin Fe^{3+} in a distorted octahedral environment. Specifically, the isomer shift (relative to natural iron) and quadrupole splitting are 0.36 and 0.87 mm·sec^{-1}, respectively. At 4.45 K, a single well resolved magnetic hyperfine pattern is observed with an internal field (H_n) value of 53.2 T, again typical of high spin Fe^{3+}. The theoretical
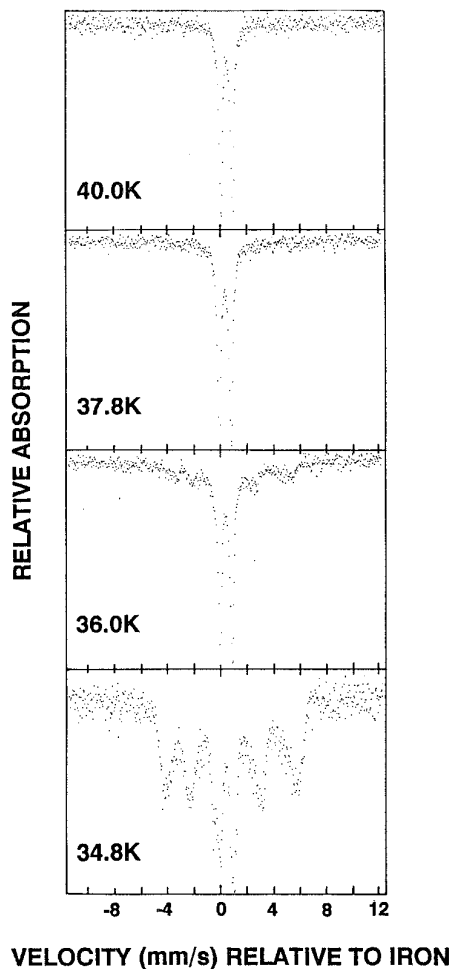

FIG. 5. $\chi(T)$ for **1**.

FIG. 7. The variable temperature ^{57}Fe Mössbauer for **1** in the vicinity of the magnetic ordering temperature.

(Fermi contact) contribution (19) to H_n is 11 T/spin or thus 55 T for high spin Fe^{3+}. Thus the observed value confirms essential magnetic saturation for the highly "ionic" FeO_6 chromophore, i.e., little reduction of H_n owing to covalency-delocalization effects.

Some sample spectra illustrating the onset of long-range three-dimensional magnetic order in the vicinity of 35 K are shown in Fig. 7. The results are consistent with the dc magnetization and ac susceptibility determinations (Figs. 8a and 8b) that also indicate a critical temperature of ca 30 K. The strong out of phase component (Fig. 8b), i.e., $\chi''_m \neq 0$, along with an overall *decrease* in μ but a sharp rise in μ precisely at $T_{Critical}$, strongly suggests a canted antiferromagnetic (3-D) magnetic ground state or alternatively so-called "weak ferromagnetism" (20). The *net moment* implied for such a ground state is clearly mirrored in the hysterisis of the dc magnetization (Fig. 9) observed at 10 K.

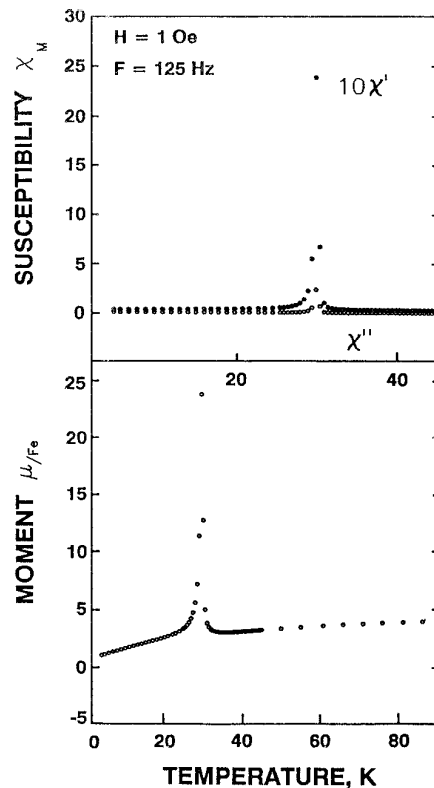The isolation and characterization of the first example

FIG. 8. The ac susceptibility (χ' and χ'') and μ/Fe for **1** as a function of temperature.

of an organically templated iron phosphate phase provides a further example that a large class of metastable phases of diverse structural type and unusual magnetic properties may be accessible within the hydrothermal reaction domain. The fact that such a large number of mineralogical examples of iron phosphates exist suggests that there
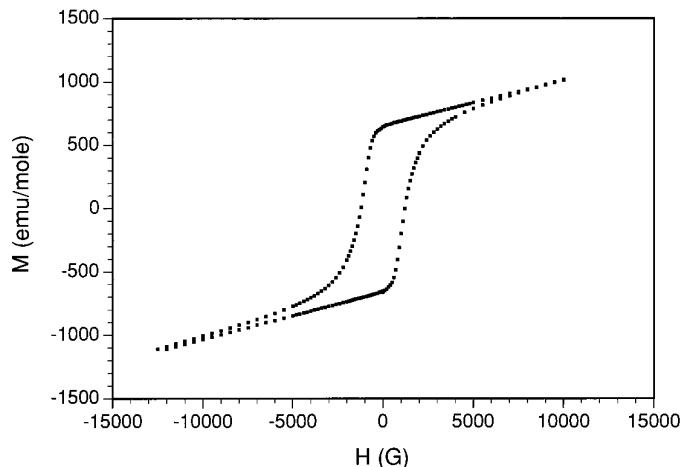

FIG. 9. The field dependence of the magnetization for **1** at 10 K.

should likewise be numerous synthetic FePO frameworks accessible, especially in light of these results which show the feasibility of incorporating structure directing organic templates. To this end, we will shortly report on the isolation and structural characterization of the first organically templated 3-D iron phosphate.

ACKNOWLEDGMENT

REFERENCES

1. R. M. Barrer, "Hydrothermal Chemistry of Zeolites." Academic Press, New York, 1982.
2. Szostak, "Molecular Sieves: Principles of Synthesis and Identification." Van Nostrand, New York, 1989.
3. J. M. Newsam, *in* "Solid State Chemistry, Compounds," (A. K. Cheetham, and P. Day, Eds.). Clarendon Press, Oxford, 1992.
4. J. Chen, R. H. Jones, S. Natajaian, M. B. Hursthouse, and J. M. Thomas, *Angew. Chem. Int. Ed. Eng.* **33,** 639 (1994).
5. C. Baerlocker, A. Merrouche, and H. Kessler, *Nature* **352,** 320 (1991).
6. R. H. Jones, J. Chen, J. M. Thomas, A. George, M. B. Hursthouse, R. Xu, S. Li, Y. Lu, and G. Yang, *Chem. Mater.* **4,** 808 (1992).
7. W. T. A. Harrison, T. E. Martin, T. E. Gier, and G. D. Stucky, *J. Mater. Chem.* **1,** 175 (1992) and references therein.
8. K.-H. Lii and C.-Y. Huang, *J. Chem. Soc., Dalton Trans.* 571 (1995); M. Gabelica-Robert, M. Goreaud, Ph. Labbe, and B. Raveau, *J. Solid State Chem.* **45,** 389 (1982); M. Pintard-Screpel, F. D'Yvoir, and J. Durand, *Acta Crystallogr. Sect. C* **39,** 9 (1983); D. Riou, Ph. Labbe, and M. Goreaud, *Eur. J. Solid State Inorg. Chem.* **25,** 215 (1988).
9. R. C. Haushalter and L. A. Mundi, *Chem. Mater.* **4,** 31 (1992) and references therein.
10. V. Soghomonian, Q. Chen, R. C. Haushalter, J. Zubieta, and C. J. O'Connor, *Science* **259,** 1596 (1993).
11. V. Soghomonian, R. C. Haushalter, Q. Chen, and J. Zubieta, *Inorg. Chem.* **33,** 1700 (1994).
12. V. Soghomonian, Q. Chen, R. C. Haushalter, C. J. O'Connor, C. Tao, and J. Zubieta, *Inorg. Chem.* **34,** 3509 (1995), and references therein.
13. D. Klissurski, V. Rives, N. Abadzlijieva, Y. Pesheva, P. Pomonis, T. Sdoukos, and D. Petrakis, *J. Chem. Soc., Chem. Commun.* 1607 (1993).
14. L. Katz and W. N. Lipscomb, *Acta Crystallogr.* **4,** 345 (1951); M. Ijjaali, B. Malaman, C. Gleitzer, J. K. Warner, J. A. Hriljac, and A. K. Cheetham, *J. Solid State Chem.* **86,** 195 (1990); C. Gleitzer, *Eur. J. Solid State Inorg. Chem.* **28,** 77 (1991); J. K. Warner, A. K. Cheetham, D. E. Cox, and R. B. Von Dreele, *J. Am. Chem. Soc.* **114,** 6074 (1992); P. D. Battle, A. K. Cheetham, C. Gleitzer, W. T. A. Harrison, G. J. Long, and G. Longworth, *J. Phys. C: Solid State Phys.* **15,** L919 (1982); J. K. Warner, A. K. Cheetham, A. G. Nord, R. B. Von Dreele, and M. Yethiraj, *J. Mater. Chem.* **2,** 191 (1992); R. J. B. Jakeman, M. J. Kwiecien, W. M. Reiff, A. K. Cheetham, and C. C. Torardi, *Inorg. Chem.* **30,** 2806 (1991).
15. P. B. Moore and A. R. Kampf, *Z. Kristallogr.* **201,** 263 (1992); P. B. Moore, *Am. Miner.* **57,** 397 (1972); P. B. Moore, *Am. Miner.* **55,** 135 (1970); P. B. Moore and T. Araki, *Inorg. Chem.* **15,** 316 (1976); P. B. Moore, "The 2nd International Congress on Phosphorus Compounds Proceedings." April 21–25, p. 105. 1980.
16. P. B. Moore and J. Shen, *Nature* **306,** 356 (1983).
17. C. Chang and W. M. Reiff, *Inorg. Chem.* **16,** 2097 (1977).
18. G. M. Bancroft, A. G. Maddock, W. K. Ong, R. H. Prince and A. J. Stone, *J. Chem. Soc. A* 1966 (1967).
19. N. N. Greenwood and T. C. Gibb, "Mössbauer Spectroscopy." Chapman and Hall, Londong, 1982.
20. W. M. Reiff, J. H. Zhang, and C. C. Torardi, *Hyperfine Interactions* **28,** 689 (1986).